



UNIVERSITY OF LEEDS

This is a repository copy of *KAI2 promotes Arabidopsis root hair elongation at low external phosphate by controlling local accumulation of AUX1 and PIN2*.

White Rose Research Online URL for this paper:

<https://eprints.whiterose.ac.uk/180315/>

Version: Accepted Version

Article:

Villaécija-Aguilar, JA, Körösy, C, Maisch, L et al. (6 more authors) (2022) KAI2 promotes Arabidopsis root hair elongation at low external phosphate by controlling local accumulation of AUX1 and PIN2. *Current Biology*, 32 (1). pp. 228-236. ISSN 0960-9822

<https://doi.org/10.1016/j.cub.2021.10.044>

© 2021, Elsevier. This manuscript version is made available under the CC-BY-NC-ND 4.0 license <http://creativecommons.org/licenses/by-nc-nd/4.0/>.

Reuse

This article is distributed under the terms of the Creative Commons Attribution-NonCommercial-NoDerivs (CC BY-NC-ND) licence. This licence only allows you to download this work and share it with others as long as you credit the authors, but you can't change the article in any way or use it commercially. More information and the full terms of the licence here: <https://creativecommons.org/licenses/>

Takedown

If you consider content in White Rose Research Online to be in breach of UK law, please notify us by emailing eprints@whiterose.ac.uk including the URL of the record and the reason for the withdrawal request.



eprints@whiterose.ac.uk
<https://eprints.whiterose.ac.uk/>

1 **KAI2 promotes root hair elongation at low**
2 **external phosphate by controlling local**
3 **accumulation of AUX1 and PIN2**
4

5 José Antonio Villaécija-Aguilar^{1,a}, Caroline Körösy¹, Lukas Maisch¹, Maxime Hamon-
6 Josse², Andrea Petrich¹, Sonja Magosch¹, Philipp Chapman¹, Tom Bennett², Caroline
7 Gutjahr^{1,*}

8
9
10 ¹Plant Genetics, TUM School of Life Sciences, Technical University of Munich (TUM),
11 Emil Ramann Str. 4, 85354 Freising, Germany.

12
13 ²School of Biology, Faculty of Biological Sciences, University of Leeds, Leeds, LS2
14 9JT, United Kingdom

15
16 ^aPresent address: LMU Munich, Faculty of Biology, Genetics, Biocenter Martinsried, 82152,
17 Martinsried, Germany.

18
19 *Lead contact: caroline.gutjahr@tum.de

20
21
22
23
24
25
26
27
28
29
30
31
32
33
34
35
36
37

38 SUMMARY

39 Root hair (RH) growth to increase the absorptive root surface area, is a key adaptation
40 of plants to limiting phosphate availability in soils. Despite the importance of this trait,
41 especially for seedling survival, little is known about the molecular events connecting
42 phosphate starvation sensing and RH growth regulation. KARRIKIN INSENSITIVE2
43 (KAI2), an α/β -hydrolase receptor of a yet-unknown plant hormone ('KAI2-ligand', KL),
44 is required for RH elongation¹. KAI2 interacts with the F-box protein MORE AXILLIARY
45 BRANCHING2 (MAX2) to target regulatory proteins of the SUPPRESSOR of MAX2 1
46 (SMAX1) family for degradation². Here we demonstrate that P_i starvation increases KL
47 signalling in Arabidopsis roots through transcriptional activation of *KAI2* and *MAX2*.
48 Both genes are required for RH elongation under these conditions, while *smax1 smx12*
49 mutants have constitutively long RHs even at high P_i availability. Attenuated RH
50 elongation in *kai2* mutants is explained by reduced shootward auxin transport from the
51 root tip resulting in reduced auxin signalling in the root hair zone, caused by an inability
52 to increase localized accumulation of the auxin importer AUXIN TRANSPORTER
53 PROTEIN1 (AUX1) and the auxin exporter PIN-FORMED2 (PIN2) upon P_i starvation.
54 Consistent with AUX1 and PIN2 accumulation being mediated via ethylene signalling³,
55 expression of *1-AMINOCYCLOPROPANE-1-CARBOXYLATE SYNTHASE 7 (ACS7)*
56 is increased at low P_i in a *KAI2*-dependent manner, and treatment with an ethylene
57 precursor restores RH elongation of *acs7* but not of *aux1* and *pin2*. Thus, KAI2
58 signalling is increased by phosphate starvation to trigger an ethylene- AUX1/PIN2-
59 auxin cascade required for RH elongation.

60

61

62

63

64

65

66

67

68

69

70 RESULTS AND DISCUSSION

71 **Root hair elongation in response to low external P_i requires KAI2**

72 Phosphorous is an essential macronutrient for plant development and growth. It is
73 taken up through the roots in the form of inorganic phosphate (P_i), which readily
74 precipitates with cations and thereby represents one of the least plant-accessible
75 nutrients in soils. Plants adapt to P_i scarcity with a number of developmental and
76 metabolic responses. An important response to P_i starvation is an increase in root hair
77 length (RHL) and density (RHD); and root hairs can be crucial for survival in low
78 phosphate soils^{4,5}.

79
80 KAI2 is an α/β -hydrolase receptor, which, upon binding of the smoke compound
81 karrikin or a yet unknown hormone, provisionally called KAI2-ligand (KL), interacts with
82 the F-box protein MAX2 to mediate the degradation of Arabidopsis SMAX1 and
83 SMXL2, thus activating downstream responses^{6,7}. In Arabidopsis, KAI2 and MAX2 are
84 required for root hair elongation at sufficient P_i availability^{1,8,9}. We examined whether
85 KAI2 signalling mediates RH elongation in response to varying external P_i levels by
86 growing KL perception and repressor mutants at three different P_i concentrations:
87 limiting P_i ('low P_i', 2 μ M P_i), sufficient P_i ('medium P_i', 625 μ M) and high P_i (2 mM P_i).
88 As a specificity control, a mutant of the strigolactone receptor D14 was included, which
89 is closely related to KAI2 and also interacts with MAX2^{10,11}. Consistent with previous
90 reports^{5,12-15}, low P_i stimulated and high P_i dampened RH elongation relative to
91 medium P_i in the wild type (Figure 1A and Figure S1A-B). The strigolactone receptor
92 mutant *d14* displayed similar RHL responses to the three P_i levels (Figure S1A),
93 indicating that strigolactone signalling is not required for this response. In contrast, the
94 RHL response to medium and low P_i is strongly attenuated in *kai2* and *max2* mutants,
95 showing that KAI2 signalling mediates root hair elongation in response to sufficient and
96 limiting P_i levels (Figure 1A and Figure S1B). SMAX1 and SMXL2 are redundant
97 proteolytic targets of KL signalling in Arabidopsis^{1,16}. Consistently, RHs of *smax1*
98 *smxl2* (*s1s2*) double mutants are longer than those of wild type in all P_i conditions.
99 Interestingly, RHL of *s1s2* mutants still responds slightly to P_i availability (Figure 1 and
100 Figure S1B), suggesting together with the slight RHL response of *kai2* and *max2* to
101 low P_i that in addition to KAI2 signalling, other pathways may contribute to the
102 response. Nevertheless, KAI2 but not strigolactone perception, is required for a major
103 portion of the RH elongation response to low external P_i availability.

104

105 To examine whether P_i starvation signalling requires KAI2 signalling, the expression
106 of the P_i starvation marker genes *PHOSPHATE TRANSPORTER 1;4* (*PHT1;4*) and
107 *INDUCED BY PHOSPHATE STARVATION 1* (*IPS1*) was analysed in *kai2* roots.
108 Transcripts of both genes increased at low P_i in a similar fashion in both wild type and
109 *kai2* roots, indicating that perception of P_i level and downstream transcriptional
110 response to P_i deficiency do not involve KAI2 (Figure 1B). We therefore reasoned that
111 KAI2 signalling might act downstream of P_i signalling. To examine whether KAI2
112 signalling in the root is itself regulated by the P_i status of the plant, the transcript levels
113 of *KAI2*, *MAX2* and *DWARF14-LIKE 2* (*DLK2*), a well-established KAI2-signalling
114 marker gene^{17,18}, were analysed. *DLK2* transcript accumulation was increased in wild-
115 type roots growing at medium and low P_i as compared to high P_i (~2.5-fold) and this
116 was dependent on *KAI2* (Figure 1B). Importantly, *KAI2* (~10-fold) and *MAX2* (~4-fold)
117 transcripts increased significantly in wild type roots grown at low versus high P_i,
118 indicating that external P_i concentration influences the transcriptional regulation of KL
119 perception components.

120 The homologous MYC transcription factors PHOSPHATE STARVATION RESPONSE
121 1 (*PHR1*) and *PHR1*-like 1 (*PHL1*) are key regulators of phosphate starvation induced
122 genes^{19,20}. We reassessed the roles of *PHR1* and *PHL1* in regulating root hair
123 elongation in response to low external P_i. Consistent with previous reports¹⁵, low P_i
124 induced an increase in RHL in wild type roots, while the root hair growth response to
125 low P_i was attenuated in *phr1 phl1* mutants, similar to *kai2* and *max2* (Figure S1C-D).
126 Importantly, the P_i-responsive transcript accumulation of *KAI2* and *DLK2* depends on
127 *PHR1 PHL1* (Figure S1E), confirming that *KAI2* transcript accumulation is activated by
128 P_i starvation in Arabidopsis roots. To further confirm that phosphate status controls
129 RHL via transcriptional regulation of *KAI2*, RHL of two lines ectopically expressing
130 *KAI2* under the *35S* promoter at the three P_i levels was examined. Both lines displayed
131 increased RHL at sufficient and high P_i and similar RHL compared to wild type at
132 limiting P_i (Figure 1C and Figure S1E), supporting that P_i starvation influences RHL by
133 inducing *KAI2* transcript accumulation. Together with the expression pattern of the
134 KAI2-signalling response gene *DLK2*, these data suggest that *KAI2* transcript
135 accumulation is translated into KAI2 protein abundance, thereby enhancing KL
136 sensitivity in response to P_i starvation.

137

138 **KAI2 promotes root hair elongation at low external P_i through ethylene**
139 **biosynthesis and signalling**

140 We recently demonstrated that SMAX1 and SMXL2 regulate root hair elongation by
141 repressing ethylene biosynthesis, via inhibition of *1-AMINOCYCLOPROPANE-1-*
142 *CARBOXYLATE SYNTHASE 7 (ACS7)* expression²¹. ACS proteins catalyse the
143 conversion of S-Adenosyl methionine to 1-aminocyclopropane-1-carboxylic acid
144 (ACC), a precursor of the plant hormone ethylene^{22,23}. *ACS7* transcript accumulation
145 is regulated by external P_i levels in a *KAI2*-dependent manner (Figure 2A).
146 Furthermore, mutation of *acs7* abolishes the RHL response to low P_i (Figure 2B).
147 Additionally, transcript levels of the essential ethylene signalling genes *ETHYLENE-*
148 *INSENSITIVE 2 (EIN2)* (encoding a protein of the ethylene receptor system) and *EIN3*
149 (encoding an ethylene responsive transcription factor) are anticorrelated with external
150 P_i concentration in wild-type but not in *kai2* mutant roots (Figure 2A, Figure S2A); and
151 *EIN2* is required for the RHL response to low P_i (Figure 2C). Moreover, the short RHL
152 of *kai2*, *max2* and *acs7* mutants is rescued by treatment with the ethylene precursor
153 ACC (Figure 2D and Figure S2B). Together this suggests that KAI2 signalling fine-
154 tunes root hair elongation in response to external P_i levels by transcriptionally
155 regulating important genes in ethylene biosynthesis (*ACS7*) and signalling (*EIN2* and
156 *EIN3*).

157

158 **KAI2 promotes shootward auxin transport**

159 Root hair elongation upon P_i starvation is driven by increased auxin signalling in the
160 epidermis of a region in which elongation and differentiation zone overlap ('E-D
161 zone')^{13,24}. We hypothesised that the *kai2* RHL phenotype may result from reduced
162 auxin signalling in this zone. To test this, the expression pattern of *DR5v2_{pro}:GFP*²⁵, a
163 transcriptional reporter for auxin response, was examined in the tips of wild type and
164 *kai2* at the three different P_i conditions. In agreement with the RHL responses and
165 previous observations¹³, *DR5v2_{pro}:GFP* expression in the epidermis of the E-D zone
166 of the wild type increases at low P_i. In contrast, in the same zone of *kai2-2* mutants
167 *DR5v2_{pro}:GFP* expression does not change across P_i conditions (Figure 3A-B, Figure
168 S3A, Data S1). Hence at low external P_i, auxin signalling increases in the E-D zone of
169 wild-type, but not of *kai2*. Conversely, in the meristem zone, P_i levels do not influence
170 *DR5v2_{pro}:GFP* expression in wild type, while *kai2-2* meristems display a significant
171 increase in GFP intensity at low P_i availability (Figure 3A, Figure S3A, Data S1). We

172 hypothesise that this may be caused by an impaired shootward auxin flow in *kai2*,
173 leading to auxin accumulation in the meristem zone, due to increased auxin
174 biosynthesis in the root tip at low P_i ¹³.

175

176 Therefore, we examined whether reduced RHL of *kai2* can be rescued by low
177 concentrations (0.5 nM and 1 nM) of exogenously applied indole-3-acetic-acid (IAA).
178 Both IAA concentrations restore RHL of *kai2* as well as *max2* mutants to the wild-type
179 level at medium P_i (Figure S3B). To understand whether *kai2-2* and *max2-1* may be
180 affected in auxin transport, auxin analogues were employed, which are substrates of
181 different types of auxin transporters. 1-naphthalene acetic acid (NAA) is a good
182 substrate for PIN-family auxin export carriers, while 2,4-dichlorophenoxyacetic acid
183 (2,4-D) tends to accumulate in cells. Conversely, influx of 2,4-D requires AUX1-family
184 auxin influx carriers, but NAA does not²⁶. Application of 1nM NAA fully restores RHL
185 of *kai2* and *max2*. However, they show a markedly reduced response to 2,4-D with no
186 additional RH elongation at 1nM and only a reduced RH elongation at 10 nM 2,4-D
187 (Figure 3C-D). To confirm this reduced 2,4-D responsiveness of *kai2*, *DR5v2_{pro}:GFP*
188 expression in root meristems of *kai2* was quantified at medium P_i . *DR5v2_{pro}:GFP*
189 expression was decreased in *kai2* meristems with respect to the wild type, possibly
190 due to reduced rootward flow of auxin through *kai2* roots²⁷. Importantly, and consistent
191 with the RHL response, *DR5v2_{pro}*-driven GFP signal in *kai2-2* increases to the level of
192 the untreated wild type after treatment with NAA, but does not change with 2,4-D
193 (Figure 3E). Together these results suggest there may be reduced influx carrier activity
194 in *kai2*. Furthermore, 1 nM NAA, but not 2,4-D, restores RHL of *ein2* mutants (Figure
195 S3C), suggesting that the reduced RHL response to 2,4-D is caused by reduced
196 ethylene signalling in *kai2* mutants, placing ethylene signalling between KL signalling
197 and auxin import in a hierarchy of regulatory steps causing RH elongation under P_i -
198 starvation^{21,28,29}. However, 1 nM 2,4-D restores RHL in *acs7* mutants (Figure S3C),
199 possibly because 2,4-D treatment may induce alternative ACS genes, thereby
200 compensating for the lack of ACS7 and boosting ethylene biosynthesis³⁰. Together,
201 these data suggest that *kai2* mutants are impaired in auxin import at low and medium
202 P_i levels, causing a reduction in shootward auxin flow to epidermal cells of the E-D
203 zone and thereby impaired RH elongation.

204

205 As 2,4-D is a substrate of the auxin importer AUX1^{31,32}, which maintains shootward
206 auxin flow from the root meristem to the E-D zone epidermis to support RH growth²⁴,
207 shootward 2,4-D transport was examined directly in wild type, *kai2*, *max2* mutants, as
208 well as the *aux1-7* mutant as a control using radiolabelled ³H-2,4-D. Consistent with a
209 role of KAI2-signalling in promoting cellular auxin import, ³H-2,4-D transport is reduced
210 in *kai2* and *max2* mutant roots (Figure 3F), suggesting that KAI2-signalling may affect
211 AUX1.

212

213 **KAI2 mediates local AUX1 accumulation in response to low external P_i**

214 AUX1 is required for the RHL response to P_i starvation^{13,33}. To understand whether an
215 altered AUX1 accumulation or distribution underlies the attenuated RHL response of
216 *kai2* to low and medium P_i, the expression of *AUX1_{pro}:AUX1-YFP* in wild type and *kai2-2*
217 mutants was analysed at the three P_i levels. The overall tissue distribution of AUX1-
218 YFP was not affected by varying P_i concentrations (Figure 4A-D, Fig. S4A, Data S1).
219 Remarkably, in the wild type AUX1-YFP intensity was increased at low P_i versus high
220 P_i in the epidermis above the lateral root cap (LRC), the LRC, the apical meristem and
221 the stele; and this increase is absent from *kai2* (Figure 4A, C, Figure S4A, Data S1).
222 Furthermore, in all investigated tissues except the root meristem, AUX1-YFP intensity
223 in *kai2* is as low across all P_i levels, as in wild type at high P_i. Also *AUX1* transcript
224 accumulation increased (~4-fold) in a *KAI2*-dependent manner in roots growing in low
225 and medium P_i as compared to high P_i (Figure S4B), suggesting that P_i-responsive
226 AUX1 accumulation may be regulated at the transcriptional level, although this remains
227 to be further investigated.

228

229 Root hair elongation requires AUX1 accumulation specifically in the LRC and the
230 epidermis just above the LRC^{13,34}. To examine whether the *KAI2*-dependent AUX1
231 accumulation in these tissues explains the RHL phenotypes of wild type and *kai2*
232 mutants, *aux1-22* mutants as well as the *aux1-22 J0951>>AUX1* enhancer trap line
233 (which expresses *AUX1* only in the lateral root cap (LRC) and root epidermal cells
234 above the LRC), were subjected to treatment with 1 μM karrikin2 (KAR₂), which triggers
235 root hair elongation in the wild type¹²¹. Neither *aux1-22* nor *aux1-22 J0951>>AUX1*
236 respond to KAR₂ treatment, showing that the KAR-response requires AUX1 and that
237 the *J0951* promoter does not respond to KAR₂ treatment (Figure 4E). However, *aux1-22*
238 *J0951>>AUX1* has an increased RHL, resembling the RH phenotype of *s1s2* and

239 supporting the idea that accumulation of AUX1 in the LRC and epidermis of the
240 differentiation zone explains KAI2-mediated root hair elongation. Indeed, in the
241 epidermis above the LRC, the LRC, apical meristem and stele of *s1s2* mutants, AUX1-
242 YFP accumulates across all P_i concentrations to similarly high levels as in the wild type
243 at low P_i (Figure 4B, D, Data S1). Thus, AUX1 accumulation in *s1s2* roots is not
244 repressed at high P_i . Furthermore, and supporting the role of AUX1 in KAI2-mediated
245 root hair elongation, *aux1-7* is epistatic to *s1s2* and fully suppresses RH elongation in
246 the triple mutant (Figure 4F). We conclude that KAI2 signalling promotes AUX1
247 accumulation in the LRC and the epidermis above at low P_i and thereby promotes
248 auxin import and RH elongation, while in *s1s2*, AUX1 accumulates in these tissues
249 independently of external P_i concentrations. This AUX1 accumulation is likely
250 regulated via KAI2-induced ethylene signalling because ethylene signalling is
251 increased in *smax1* mutants of *Lotus japonicus*²¹, Arabidopsis AUX1 accumulates in
252 the LRC upon ACC treatment and is required for ACC induced primary root growth
253 inhibition^{29,35}, and ACC treatment does not restore root hair elongation in *aux1-22*
254 (Figure S4C).

255

256 **KAI2 mediates local PIN2 accumulation at low, but does not explain its increase** 257 **at high external P_i**

258 Similar to AUX1, the auxin exporter PIN-FORMED2 (PIN2) contributes to root hair
259 elongation at low P_i and PIN2-GFP accumulates in response to ACC^{35,38}. We used
260 *ethylene insensitive root 1 (eir1-1/pin2)* mutants to examine, whether *PIN2* is required
261 for root hair elongation in response to KAR₂ and ACC at medium P_i . As previously
262 reported for *pin2*, *eir1-1* had shorter RHL than the wild type³⁸, moreover, it did not
263 respond to KAR₂ and ACC (Figure S4D, E), showing that PIN2 is required for the RHL
264 response to these compounds. Unlike *AUX1*, the *PIN2* transcript level in roots did not
265 change among genotypes or in response to P_i (Figure S4B). However, at all P_i levels
266 PIN2-GFP (expressed as *PIN2_{pro}:PIN2-GFP*) accumulated significantly less in root tips
267 of *kai2* as compared to wild type (Figure 4G, H), indicating a requirement of KAI2 for
268 proper PIN2 protein accumulation. In contrast to AUX1-YFP, PIN2-GFP levels
269 significantly increased at medium and high P_i in the meristematic zone at 150-300 μ M
270 distance from the root tip in wild type. This was also observed by³⁹ and could indicate
271 a necessity for increase PIN2 levels to remove auxin from the elongation zone to
272 disable root hair elongation. Consistent with this hypothesis, 35S promoter-based

273 overexpression of *PIN2* causes a reduction in RHL⁴⁰. *PIN2*-GFP intensity also
274 increased in *kai2* at high P_i, indicating that this increase is at least partially independent
275 of *KAI2* signalling.

276

277

278 In summary, we have established a mechanistic framework by which *KAI2* signalling
279 regulates RH elongation in response to low external P_i (Figure 4G). Upon P_i starvation
280 *KAI2* and *MAX2* are transcriptionally activated through previously defined P_i signalling
281 pathways, likely increasing the sensitivity to KL. The consequent increased
282 degradation of *SMAX1* and *SMXL2* releases repression of *ACS7* expression, thereby
283 enhancing ethylene synthesis and signalling in the root. This causes an increase of
284 *AUX1* accumulation in the RLC and the epidermis above, as well as an accumulation
285 of *PIN2* in the meristematic and elongation zones, together allowing increased auxin
286 transport to the E-D zone and a boost in RH elongation. Consistent with this model,
287 *KAR₂*, *ACC* and *NAA* promote RHL at high P_i in the wild type (Figure S4F). It was
288 recently shown that the transcription factor dimer TARGET OF
289 MONOPTEROS5/LONESOME HIGHWAY (*TMO5/LSW*) regulates RHL and density
290 from the xylem via cytokinin signalling⁴¹. It will be interesting to understand whether
291 this regulatory module participates in the hormonal cascade presented here or whether
292 it acts independently for example accounting for the residual RHL response to low P_i
293 observed in karrikin perception mutants. It will now be important to understand how
294 *KAI2* and *MAX2* expression is regulated in response to external P_i, and which
295 transcriptional regulators activate the *ACS7* and *AUX1* promoters in response to *KAI2*-
296 and ethylene-signalling, respectively. Furthermore, once the KL has been identified, it
297 will be interesting to determine, whether its biosynthesis is regulated in response to P_i
298 availability, similar to strigolactone synthesis in crop plants^{36,37}.

299

300 ACKNOWLEDGMENTS

301 We are grateful to Laura Mesa Estrada, Antonina Shlykova and Patrick Wiesbeck for
302 excellent technical support. We thank Ranjan Swarup (University of Nottingham, UK)
303 for *aux1-22 J0951* and *aux1-22 J0951>>AUX1* seeds, Javier Paz-Ares (CSIC National
304 Center for Biotechnology, Madrid, Spain) for *phr1 phl1* seeds, and Mark T. Waters
305 (University of Western Australia, Australia) for seeds of *35S_{pro}:KAI2* lines. We thank
306 Ralph Hückelhoven for granting access to his confocal microscope and the Center for

307 Advanced Light Microscopy (CALM) of the TUM School of Life Sciences for support.
308 This study was funded by the Emmy Noether Program of the Deutsche
309 Forschungsgemeinschaft (Grant GU1423/1-1) to CG and by the BBSRC
310 (BB/R00398X/1) to TB. CK was supported by a doctoral student fellowship of the
311 Cusanuswerk.

312

313 AUTHOR CONTRIBUTIONS

314 JAVA, TB and CG designed the study. JAVA, CK, MHJ, TB and CG planned
315 experiments and analysed data. JAVA, CK, LM, MHJ, AP, SM, PC and TB carried out
316 experiments. JAVA prepared all figures and performed statistical analyses. JAVA and
317 CG wrote the manuscript with input from all authors. TB and CG provided mentoring
318 and supervision. CK, TB and CG acquired funding.

319

320 DECLARATION OF INTERESTS

321 The authors declare they have no competing interests.

322

323 MAIN FIGURE TITLES AND LEGENDS

324

325 **Figure 1. Root hair elongation in response to low external P_i requires KAI2.**

326 (A) Root hair length in Col-0 wild type and karrikin signalling mutants at low (LP, 2 μ M),
327 medium (MP, 625 μ M) or high (HP, 2000 μ M) external P_i . n = 10. This result was
328 obtained in 2 independent experiments. (B) Transcript accumulation of indicated genes
329 in Col-0 wild type and *kai2-2* mutant roots at LP, MP and HP. Expression levels were
330 normalized with those of *UBIQUITIN10*, n = 4 biological replicates. Red lines indicate
331 the means. (C) Root hair length in *Ler* wild type, *kai2* and *35S:KAI2* lines (all in *Ler*
332 background) at low (LP, 2 μ M), medium (MP, 625 μ M) or high (HP, 2000 μ M) external
333 P_i . n = 10. A, C: these results were obtained in 2 independent experiments. Different
334 letters indicate different statistical groups (Kruskal-Wallis test with post-hoc Student's
335 t-test, $p \leq 0.05$). See also Figure S1.

336

337 **Figure 2. KAI2 promotes root hair elongation at low external P_i through ethylene biosynthesis and signalling.**

338 (A) Transcript accumulation of *EIN2* and *ACS7* in Col-0 wild type and *kai2-2* mutant
339 roots at low (LP, 2 μ M), medium (MP, 625 μ M) or high (HP, 2000 μ M) external P_i .
340 Expression levels were normalized with those of *UBIQUITIN10*, n = 4 biological
341 replicates. Red lines indicate the means. (B-C) Root hair length of indicated genotypes
342 at LP, MP and HP n = 10. (D) Root hair length of indicated genotypes at MP and treated
343 with solvent, 1 nM ACC, 10 nM ACC or 100 nM ACC, n = 10. (B-D) Results were
344 obtained in 2 independent experiments. Different letters indicate different statistical
345 groups (Kruskal-Wallis test with post-hoc Student's t-test, $p \leq 0.05$). See also Figure S2.

346

347 **Figure 3. KAI2 controls changes in auxin response in the root hair initiation zone at low external P_i and promotes shootward auxin transport.**

348

350 (A) Fluorescence intensity (AU, arbitrary units) of nuclear localized GFP derived from
351 *DR5v2_{pro}:GFP* in the zone, in which elongation and differentiation zone overlap (E-D
352 zone) and the apical meristem of Col-0 wild type and *kai2-2* at low (LP, 2 μ M), medium
353 (MP, 625 μ M) or high (HP, 2000 μ M) external P_i . n = 6 roots were used per image (B)
354 Representative images of E-D zone used for fluorescence measurements in Figure
355 3A. Scale bar, 100 μ m. (C-D) Root hair length of Col-0 wild type, *kai2-2* and *max2-1* at
356 MP treated with (C) solvent, 1 nM or 10 nM NAA, and (D) solvent, 1 nM or 10 nM 2,4-
357 D, n = 10. (A-D) Results were obtained in 2 independent experiments. (E)
358 Fluorescence intensity (AU) of nuclear localized GFP derived from *DR5v2_{pro}:GFP* in
359 the apical meristem of Col-0 wild type and *kai2-2* roots at MP and treated with solvent,
360 1 nM NAA, 10 nM NAA, 1 nM 2,4-D or 10 nM 2,4-D, n = 6. This result was obtained in
361 2 independent experiments. (F) Shootward 3 H-2,4-D transport detected in 5 mm long
362 root segments between 2 and 7 mm from the root tip of *aux1-7*, *kai2-2* and *max2-1*, n
363 = 8. Results are representative for 2 independent experiments. Different letters indicate
364 different statistical groups (Kruskal-Wallis test with post-hoc Student's t-test, $p \leq 0.05$).
365 See also Figure S3 and Data S1.
366

367 **Figure 4. KAI2 mediates local AUX1 accumulation in response to low external P_i .**
368 (A-B) Fluorescence intensity (AU, arbitrary units) of AUX1-YFP derived from
369 *AUX1_{pro}:AUX1-YFP* of (A) Col-0 wild type and *kai2-2* and (B) of Col-0 wild type and
370 *s1s2* in the epidermis above the lateral root cap (RLC), the RLC, the stele and the
371 apical root meristem at low (LP, 2 μ M), medium (MP, 625 μ M) or high (HP, 2000 μ M)
372 external P_i . For root regions used for measurement, see Figure S4A. These results
373 were obtained in 2 (A) and 1 (B) independent experiment(s), n = 6. (C-D)
374 Representative images from A and B. Scale bar, 40 μ m. (E) Root hair length of Col-0
375 wild type, *aux1-22* J0951 and *aux1-22* J0951>>AUX1 at MP and treated with solvent
376 or 1 μ M karrikin2 (KAR₂), n = 10. (F) Root hair length of Col-0 wild type, *s1s2*, *aux1-7*
377 and *s1s2 aux1-7* triple mutants at MP, n = 10. (E-F) Results were obtained in 2
378 independent experiments. (G) Fluorescence intensity (AU, arbitrary units) of PIN2-
379 GFP derived from *PIN2_{pro}:PIN2-GFP* of Col-0 wild type and *kai2-1* in the elongation
380 and meristematic zone at low (LP, 2 μ M), medium (MP, 625 μ M) or high (HP, 2000 μ M)
381 external P_i . For root regions used for measurement, see Figure S4F. These results
382 were obtained in 1 independent experiment, n = 6. (H) Representative images from G.
383 Scale bar, 50 μ m. n = 6. (A-B, E-G) Different letters indicate different statistical groups
384 (Kruskal-Wallis test with post-hoc Student's t-test, $p \leq 0.05$). (I) Proposed model for the
385 control of root hair elongation at different P_i levels. At low external phosphate, KAI2
386 expression is increased leading to higher KAI2 accumulation and KL sensitivity. Upon
387 KL perception, abundant KAI2 promotes the degradation of the repressor proteins
388 SMAX1 and SMXL2. This releases the suppression of ACS7 expression and increases
389 ethylene biosynthesis and signalling. Increased ethylene signalling boosts the
390 accumulation of AUX1 (magenta) in the LRC and epidermis above, and of PIN2 (green)
391 in the meristematic and elongation zone, increasing the shootward auxin flux to the E-
392 D zone (zone in which elongation and differentiation zone overlap). Increased auxin
393 availability (*DR5v2_{pro}* -activity shown in blue) in the E-D zone promotes root hair
394 elongation. At high P_i , KAI2 expression, KAI2 accumulation and KL sensitivity are
395 reduced. Thus, degradation of SMAX1 and SMXL2 is low and they can accumulate,
396 repress ACS7 expression and thereby ethylene biosynthesis and signalling.
397 Consequently, AUX1 in the LRC and epidermis above accumulates at low levels,
398 resulting in low auxin flow to the E-D zone and reduced root hair elongation. In contrast
399 to AUX1, PIN2 protein abundance increases, possibly promoting removal of auxin from
400 the E-D zone. This increase is independent of KAI2 and regulated by an unknown

401 factor (X) and mechanism indicated by a question mark. See also Figure S4 and Data
402 S1.
403

404 **STAR Methods**

405 Resource Availability

406 **Lead Contact and Material Availability**

407 Further information and requests for resources and reagents should be directed to and
408 will be fulfilled by the Lead Contact, Caroline Gutjahr (caroline.gutjahr@tum.de).

409 **Data and Code Availability**

410 This study did not generate any new dataset or code.
411

412 Experimental Model and Subject Details

413 **Plant material and growth conditions**

414 *Arabidopsis thaliana* ecotype Columbia-0 (Col-0) and Landsberg erecta (Ler) were
415 used in this study. The *kai2-1* and *kai2-2* mutants were originally in Landsberg *erecta*
416 (Ler) background and were backcrossed six times to Col-0⁴⁴. New genotypes were
417 generated by crossing the existing genotypes (see resource table) and homozygous
418 lines were identified using PCR genotyping (see table S1 for primers) and fluorescent
419 protein markers.

420 *Arabidopsis thaliana* seeds were surface sterilized by washing with 1 ml of 70% (v/v)
421 ethanol and 0.05% (v/v) Triton X-100 with gentle mixing by inversion for 6 minutes at
422 room temperature, followed by 1 wash with 96% ethanol and 5 washes with sterile
423 distilled water. Seedlings were grown in axenic conditions on 12x12cm square Petri
424 dishes containing 60 ml 0.5x Murashige & Skoog medium, pH5.8 (½ MS) (Duchefa,
425 Netherlands), supplemented with 1% sucrose. For P_i variability experiments, the 0.5x
426 Murashige & Skoog medium was modified with low (2 μM), sufficient (625 μM) or high
427 (2 mM) P_i with KH₂PO₄, and potassium concentrations were adjusted with KCl. Seeds
428 were stratified at 4°C for 2-3 days in the dark, and then transferred to a growth cabinet
429 GroBanks (CLF Plant Climatics, Wertingen Germany), model BB-XXL.3 with 22 °C,
430 16-h/8-h light/dark cycle (intensity ~120 μmol m⁻² s⁻¹) and placed in vertical position.

431

432 Method Details

433 **Phytohormone treatments**

434 NAA and 2,4-D were dissolved in 2% DMSO and 70% ethanol respectively for Figure
435 3E. For all other experiments, NAA, 2,4-D or IAA were dissolved in either 70% ethanol
436 or 100% ethanol for the preparation of 1mM or 10 mM stock solutions, respectively. 1
437 mM stock solution of KAR₂ was prepared in 70% methanol. For root hair elongation
438 experiments the volume of these stock solutions required to reach the final
439 concentration was added to molten agar media prior to pouring Petri dishes. In each
440 experiment, an equal volume of solvent was added to the media for untreated controls.

441

442 **Determination of root hair length**

443 Images of 10 seedling roots per genotype and treatment were taken 5 days after
444 placing seeds into the light with a Zeiss Discovery V8 microscope equipped with a
445 Zeiss Axiocam 503 camera. Root hair length was measured for 10 different root hairs
446 per root, between 2 and 3 mm from the root tip using Fiji
447 (<https://imagej.net/Fiji/Downloads>) according to⁴².

448

449 **Confocal microscopy**

450 Laser-scanning confocal microscopy for *DR5v2_{pro}:GFP* was performed with a 10x or
451 20x lens using a Zeiss LSM700, LSM880 (for Figure 3E), or Leica TCS SP5 or SP8
452 imaging system for all other experiments. GFP was excited using a 488 nm laser, and
453 fluorescence was detected between 488 and 555nm. Roots were stained with
454 propidium iodide (10 µg/ml) and mounted on slides. Propidium iodide was excited with
455 a 561 nm laser, and fluorescence was detected above 610nm. For AUX1-YFP and
456 PIN2-GFP laser-scanning confocal microscopy a Leica TCS SP5 or SP8 imaging
457 system with 10X or 20X lens was used. YFP was excited using a 514 nm laser, and
458 fluorescence was detected between 520 and 550nm. The same laser power and
459 detection settings were used for all images captured in a single experiment. GFP and
460 YFP quantification was performed on non-saturated images using Fiji.

461

462 **RNA extraction and gene expression analysis**

463 For RT-qPCR analysis, a minimum of 80 roots per sample from 5 days old seedlings
464 was rapidly shock frozen in liquid nitrogen. RNA was extracted using NucleoSpin RNA
465 plant and fungi kit (Macherey-Nagel). The concentration and purity of RNA was
466 evaluated with a DS-11 FX+ spectrophotometer/fluorometer (DeNovix). 500 ng RNA

467 was used for cDNA synthesis. First-strand cDNA was produced in a 20 μ L reaction
468 volume using iScript (Biorad) with an optimized blend of oligodT and random primers.

469

470 The cDNA was diluted with water in a 1:10 ratio and 2 μ L of this solution was used for
471 RT-qPCR in a 7 μ L reaction volume using 3.3 μ L of the EvaGreen Mastermix
472 (Metabion, UNG+/ROX+ 2x conc.) and 0.85 μ L of each primer (10 μ M stocks) shown
473 in Supplementary Table 1. The qPCR reactions were carried out using a CFX384
474 Touch™ RT-PCR detection system (Bio-Rad). Thermal cycler conditions were: 95°C
475 2 min, 40 cycles of 95°C 30s, 60°C 30s and 72°C 20 s, followed by dissociation curve
476 analysis. Expression levels were calculated using the $\Delta\Delta$ Ct method⁴³. For each
477 genotype 3 or 4 biological replicates (see Figure legends for more details) were
478 analysed and each sample was represented by 3 technical replicates.

479

480 **Auxin transport assay**

481 For the auxin transport assay, an agar droplet containing 100 nM ³H-2,4-D was applied
482 on the root tip of Arabidopsis seedlings 5 days post germination. 18 hours after the
483 treatment, the amount of radioactivity was quantified in 5 mm long segments from 2 to
484 7 mm from the root tip and above the agar drop as previously described in⁴⁴.

485

486 **Accession numbers**

487 Sequence data for the genes mentioned in this article can be found in The Arabidopsis
488 Information Resource (TAIR; <https://www.arabidopsis.org>) under the following
489 accession numbers: *PHT1:4*, AT2G38940; *IPS1*, AT3G09922; *KAI2*, AT4G37470;
490 *MAX2*, AT2G42620; *DLK2*, AT3G24420, *AUX1*, AT2G38120; *ACS7*, AT4G26200;
491 *EIN2*, AT5G03280; *EIN3*, AT3G20770.

492

493 **Quantification and Statistical Analysis**

494 Statistical analyses were performed in R-studio using the package *agricolae*.
495 Significant differences were tested using Kruskal-Wallis test with post-hoc Student's t-
496 test.

497

498 **REFERENCES**

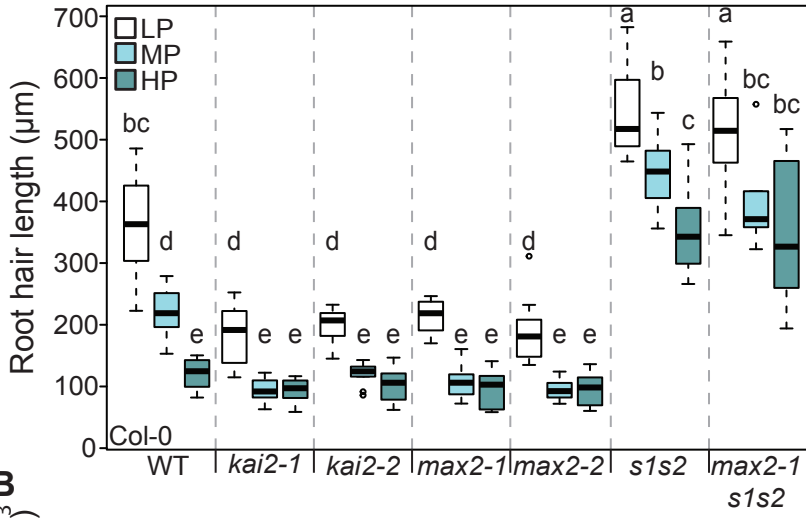
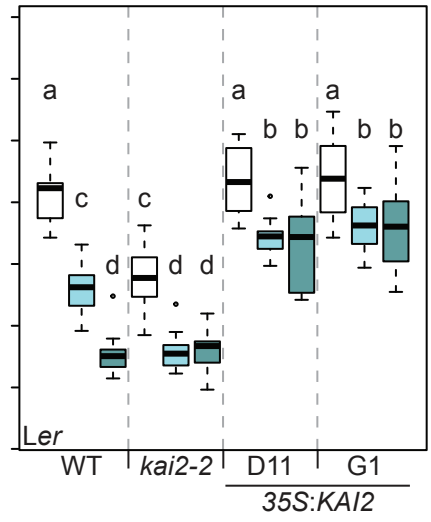
499 1. Villaécija-Aguilar, J.A., Hamon-Josse, M., Carbonnel, S., Kretschmar, A.,
500 Schmidt, C., Dawid, C., Bennett, T., and Gutjahr, C. (2019). SMAX1/SMXL2

- 501 regulate root and root hair development downstream of KAI2-mediated
502 signalling in Arabidopsis. PLOS Genet. 15, e1008327.
- 503 2. Machin, D.C., Hamon-Josse, M., and Bennett, T. (2020). Fellowship of the rings:
504 a saga of strigolactones and other small signals. New Phytol. 225, 621-636.
- 505 3. Růžička, K., Šimášková, M., Duclercq, J., Petrášek, J., Zažímalová, E., Simon,
506 S., Friml, J., Van Montagu, M.C.E., and Benková, E. (2009). Cytokinin regulates
507 root meristem activity via modulation of the polar auxin transport. Proc. Natl.
508 Acad. Sci. USA. 106, 4284-4289.
- 509 4. Gahoonia, T.S., and Nielsen, N.E. (2003). Phosphorus (P) uptake and growth
510 of a root hairless barley mutant (*bald root barley, brb*) and wild type in low- and
511 high-P soils. Plant Cell Environ. 26, 1759-1766.
- 512 5. López-Bucio, J., Hernández-Abreu, E., Sánchez-Calderón, L., Nieto-Jacobo, M.
513 F., Simpson, J., and Herrera-Estrella, L. (2002). Phosphate availability alters
514 architecture and causes changes in hormone sensitivity in the Arabidopsis root
515 system. Plant Physiol. 129, 244-256.
- 516 6. Khosla, A., Morffy, N., Li, Q., Faure, L., Chang, S.H., Yao, J., Zheng, J., Cai,
517 M.L., Stanga, J.P., Flematti, G.R., et al. (2020). Structure-function analysis of
518 SMAX1 reveals domains that mediate its karrikin-induced proteolysis and
519 interaction with the receptor KAI2. Plant Cell, 32, 2639-2659.
- 520 7. Wang, L., Xu, Q., Yu, H., Ma, H., Li, X., Yang, J., Chu, J., Xie, Q., Wang, Y.,
521 Smith, S.M., et al. (2020). Strigolactone and karrikin signaling pathways elicit
522 ubiquitination and proteolysis of SMXL2 to regulate hypocotyl elongation in
523 *Arabidopsis thaliana*. Plant Cell, 32, 2251-2270.
- 524 8. Kapulnik, Y., Delaux, P.-M., Resnick, N., Mayzlish-Gati, E., Winer, S.,
525 Bhattacharya, C., Séjalon-Delmas, N., Comber, J.-P., Bécard, G., Belausov,
526 E., et al. (2011). Strigolactones affect lateral root formation and root-hair
527 elongation in Arabidopsis. Planta 233, 209-216.
- 528 9. Kapulnik, Y., Resnick, N., Mayzlish-Gati, E., Kaplan, Y., Winer, S.,
529 Hershenhorn, J., and Koltai, H. (2011). Strigolactones interact with ethylene and
530 auxin in regulating root-hair elongation in Arabidopsis. J. Exp. Bot. 62, 2915-
531 2924.
- 532 10. Hamiaux, C., Drummond, R.S., Janssen, B.J., Ledger, S.E., Cooney, J.M.,
533 Newcomb, R.D., and Snowden, K.C.J. (2012). DAD2 is an α/β hydrolase likely
534 to be involved in the perception of the plant branching hormone, strigolactone.
535 Curr. Biol. 22, 2032-2036.
- 536 11. Bythell-Douglas, R., Rothfels, C.J., Stevenson, D.W.D., Graham, S.W., Wong,
537 G.K.-S., Nelson, D.C., and Bennett, T. (2017). Evolution of strigolactone
538 receptors by gradual neo-functionalization of KAI2 paralogues. BMC Biol. 15,
539 52.
- 540 12. Bates, T.R., and Lynch, J.P. (1996). Stimulation of root hair elongation in
541 *Arabidopsis thaliana* by low phosphorus availability. Plant Cell Environ. 19, 529-
542 538.
- 543 13. Bhosale, R., Giri, J., Pandey, B.K., Giehl, R.F.H., Hartmann, A., Traini, R.,
544 Truskina, J., Leftley, N., Hanlon, M., Swarup, K., et al. (2018). A mechanistic
545 framework for auxin dependent Arabidopsis root hair elongation to low external
546 phosphate. Nat. Commun. 9, 1409.
- 547 14. Müller, M., and Schmidt, W. (2004). Environmentally induced plasticity of root
548 hair development in Arabidopsis. Plant Physiol. 134, 409-419.
- 549 15. Bustos, R., Castrillo, G., Linhares, F., Puga, M.I., Rubio, V., Pérez-Pérez, J.,
550 Solano, R., Leyva, A., and Paz-Ares, J. (2010). A central regulatory system

- 551 largely controls transcriptional activation and repression responses to
552 phosphate starvation in Arabidopsis. PLoS Genet. 6, e1001102.
- 553 16. Stanga, J.P., Morffy, N., and Nelson, D.C. (2016). Functional redundancy in the
554 control of seedling growth by the karrikin signaling pathway. Planta 243, 1397-
555 1406.
- 556 17. Waters, M.T., Nelson, D.C., Scaffidi, A., Flematti, G.R., Sun, Y.K., Dixon, K.W.,
557 and Smith, S.M. (2012). Specialisation within the DWARF14 protein family
558 confers distinct responses to karrikins and strigolactones in Arabidopsis.
559 Development 139, 1285-1295.
- 560 18. Sun, H., Tao, J., Gu, P., Xu, G., and Zhang, Y. (2016). The role of strigolactones
561 in root development. Plant Signal. Behav. 11, e1110662-e1110662.
- 562 19. Puga, M.I., Mateos, I., Charukesi, R., Wang, Z., Franco-Zorrilla, J.M., de
563 Lorenzo, L., Irigoyen, M.L., Masiero, S., Bustos, R., Rodríguez, J., et al. (2014).
564 SPX1 is a phosphate-dependent inhibitor of PHOSPHATE STARVATION
565 RESPONSE 1 in Arabidopsis. Proc. Natl. Acad. Sci. USA. 111, 14947-14952.
- 566 20. Qi, W., Manfield, I.W., Muench, S.P., and Baker, A. (2017). AtSPX1 affects the
567 AtPHR1-DNA-binding equilibrium by binding monomeric AtPHR1 in solution.
568 Biochem. J. 474, 3675-3687.
- 569 21. Carbonnel, S., Das, D., Varshney, K., Kolodziej, M.C., Villaécija-Aguilar, J.A.,
570 and Gutjahr, C. (2020). The karrikin signaling regulator SMAX1 controls *Lotus*
571 *japonicus* root and root hair development by suppressing ethylene biosynthesis.
572 Proc. Natl. Acad. Sci. USA. 117, 21757-21765.
- 573 22. Chae, H.S., and Kieber, J.J. (2005). Eto Brute? Role of ACS turnover in
574 regulating ethylene biosynthesis. Trends Plant Sci. 10, 291-296.
- 575 23. Yamagami, T., Tsuchisaka, A., Yamada, K., Haddon, W.F., Harden, L.A., and
576 Theologis, A. (2003). Biochemical diversity among the 1-amino-cyclopropane-
577 1-carboxylate synthase isozymes encoded by the Arabidopsis gene family. J.
578 Biol. Chem. 278, 49102-49112.
- 579 24. Jones, A.R., Kramer, E.M., Knox, K., Swarup, R., Bennett, M.J., Lazarus, C.M.,
580 Leyser, H.M.O., and Grierson, C.S. (2009). Auxin transport through non-hair
581 cells sustains root-hair development. Nat. Cell Biol 11, 78-84.
- 582 25. Liao, C.-Y., Smet, W., Brunoud, G., Yoshida, S., Vernoux, T., and Weijers, D.
583 (2015). Reporters for sensitive and quantitative measurement of auxin
584 response. Nat. Methods 12, 207-210.
- 585 26. Ma, Q., Grones, P., and Robert, S. (2018). Auxin signaling: a big question to be
586 addressed by small molecules. J. Exp. Bot. 69, 313-328.
- 587 27. Hamon-Josse, M., Villaecija-Aguilar, J., Ljung, K., Leyser, O., Gutjahr, C., and
588 Bennett, T. (2021). KAI2 regulates seedling development by mediating light-
589 induced remodelling of auxin transport. bioRxiv 443001.
- 590 28. Strader, L.C., Culler, A.H., Cohen, J.D., and Bartel, B. (2010). Conversion of
591 endogenous indole-3-butyric acid to indole-3-acetic acid drives cell expansion
592 in Arabidopsis seedlings. Plant Physiol. 153, 1577-1586.
- 593 29. Liu, M., Zhang, H., Fang, X., Zhang, Y., and Jin, C. (2018). Auxin acts
594 downstream of ethylene and nitric oxide to regulate magnesium deficiency-
595 induced root hair development in *Arabidopsis thaliana*. Plant Cell Physiol. 59,
596 1452-1465.
- 597 30. Song, Y. (2014). Insight into the mode of action of 2,4-dichlorophenoxyacetic
598 acid (2,4-D) as an herbicide. J. Int. Plant Biol. 56, 106-113.
- 599 31. Yang, Y., Hammes, U.Z., Taylor, C.G., Schachtman, D.P., and Nielsen, E.
600 (2006). High-affinity auxin transport by the AUX1 influx carrier protein. Curr.
601 Biol. 16, 1123-1127.

- 602 32. Hoyerova, K., Hosek, P., Quareshy, M., Li, J., Klima, P., Kubes, M., Yemm,
603 A.A., Neve, P., Tripathi, A., Bennett, M.J., et al. (2018). Auxin molecular field
604 maps define AUX1 selectivity: many auxin herbicides are not substrates. *New*
605 *Phytol.* *217*, 1625-1639.
- 606 33. Giri, J., Bhosale, R., Huang, G., Pandey, B.K., Parker, H., Zappala, S., Yang,
607 J., Dievart, A., Bureau, C., Ljung, K., et al. (2018). Rice auxin influx carrier
608 OsAUX1 facilitates root hair elongation in response to low external phosphate.
609 *Nat. Commun.* *9*, 1408.
- 610 34. Swarup, R., Kramer, E.M., Perry, P., Knox, K., Leyser, H.M., Haseloff, J.,
611 Beemster, G.T., Bhalerao, R., and Bennett, M.J. (2005). Root gravitropism
612 requires lateral root cap and epidermal cells for transport and response to a
613 mobile auxin signal. *Nat. Cell Biol.* *7*, 1057-1065.
- 614 35. Růžička, K., Ljung, K., Vanneste, S., Podhorská, R., Beeckman, T., Friml, J.,
615 and Benková, E. (2007). Ethylene regulates root growth through effects on
616 auxin biosynthesis and transport-dependent auxin distribution. *Plant Cell* *19*,
617 2197-2212.
- 618 36. López-Ráez, J.A., Charnikhova, T., Gómez-Roldán, V., Matusova, R., Kohlen,
619 W., De Vos, R., Verstappen, F., Puech-Pages, V., Bécard, G., Mulder, P., et al.
620 (2008). Tomato strigolactones are derived from carotenoids and their
621 biosynthesis is promoted by phosphate starvation. *New Phytol.* *178*, 863-874.
- 622 37. Yoneyama, K., Xie, X., Kisugi, T., Nomura, T., and Yoneyama, K. (2013).
623 Nitrogen and phosphorus fertilization negatively affects strigolactone production
624 and exudation in sorghum. *Planta* *238*, 885-894.
- 625 38. Lin, D. L., Yao, H. Y., Jia, L. H., Tan, J. F., Xu, Z. H., Zheng, W. M., & Xue, H.
626 W. (2020). Phospholipase D-derived phosphatidic acid promotes root hair
627 development under phosphorus deficiency by suppressing vacuolar
628 degradation of PIN-FORMED2. *New Phytol.* *226*, 142-155.
- 629 39. Kumar, M., Pandya-Kumar, N., Dam, A., Haor, H., Mayzlish-Gati, E., Belausov,
630 E., Wininger, S., Abu-Abied, M., McErlean, C. S., Bromhead, L. J., et al. (2015).
631 *Arabidopsis* response to low-phosphate conditions includes active changes in
632 actin filaments and PIN2 polarization and is dependent on strigolactone
633 signalling. *J. Exp. Bot.* *66*, 1499–1510.
- 634 40. Ganguly, A., Lee, S. H., Cho, M., Lee, O. R., Yoo, H., & Cho, H. T. (2010).
635 Differential auxin-transporting activities of PIN-FORMED proteins in
636 *Arabidopsis* root hair cells. *Plant Physiol.* *153*, 1046–1061.
- 637 41. Wendrich, J. R., Yang, B., Vandamme, N., Verstaen, K., Smet, W., Van de
638 Velde, C., Minne, M., Wybouw, B., Mor, E., Arents, H. E., et al. (2020). Vascular
639 transcription factors guide plant epidermal responses to limiting phosphate
640 conditions. *Science* *370*, eaay4970.
- 641 42. Villaécija-Aguilar JA, Struk S, Goormachtig S, Gutjahr C (2021) Bioassays for
642 the effect of strigolactones and other small molecules on root and root hair
643 development. *Methods in Molecular Biology* 2309: 129-142. In: Prandi C,
644 Cardinale F (eds.) *Strigolactones: Methods and Protocols*. Springer Nature,
645 Switzerland.
- 646 43. Czechowski, T., Bari, R.P., Stitt, M., Scheible, W.R., and Udvardi, M.K. (2004).
647 Real-time RT-PCR profiling of over 1400 *Arabidopsis* transcription factors:
648 unprecedented sensitivity reveals novel root- and shoot-specific genes. *Plant J.*
649 *38*, 366-379.
- 650 43. Lewis, D.R., and Muday, G.K. (2009). Measurement of auxin transport in
651 *Arabidopsis thaliana*. *Nature Prot.* *4*, 437-451.

- 652 44. Bennett, T., Liang, Y., Seale, M., Ward, S., Müller, D., and Leyser, O. (2016).
653 Strigolactone regulates shoot development through a core signalling pathway.
654 Biol. Open 5, 1806-1820.
- 655 45. Nelson, D. C., Scaffidi, A., Dun, E. A., Waters, M. T., Flematti, G. R., Dixon, K.
656 W., Beveridge, C. A., Ghisalberti, E. L., & Smith, S. M. (2011). F-box protein
657 MAX2 has dual roles in karrikin and strigolactone signaling in *Arabidopsis*
658 *thaliana*. Proc. Natl. Acad. Sci. USA. 108, 8897-902.
- 659 46. Stirnberg, P., van De Sande, K., and Leyser, H.M. (2002). MAX1 and MAX2
660 control shoot lateral branching in Arabidopsis. Development 129, 1131-1141.
- 661 47. Alonso, J.M., Hirayama, T., Roman, G., Nourizadeh, S., and Ecker, J.R. (1999).
662 EIN2, a bifunctional transducer of ethylene and stress responses in
663 Arabidopsis. Science 284, 2148-2152.
- 664 48. Pickett, F.B., Wilson, A.K., and Estelle, M. (1990). The *aux1* mutation of
665 Arabidopsis confers both auxin and ethylene resistance. Plant Physiol. 94,
666 1462-1466.
- 667 49. Waters, M. T., Scaffidi, A., Moulin, S. L., Sun, Y. K., Flematti, G. R., & Smith, S.
668 M. (2015). A *Selaginella moellendorffii* ortholog of KARRIKIN INSENSITIVE2
669 functions in Arabidopsis development but cannot mediate responses to karrikins
670 or strigolactones, Plant Cell 27, 1925–1944.
- 671 50. Swarup, R., Kargul, J., Marchant, A., Zadik, D., Rahman, A., Mills, R., Yemm,
672 A., May, S., Williams, L., Millner, P., et al. (2004). Structure-function analysis of
673 the presumptive Arabidopsis auxin permease AUX1. Plant Cell 16, 3069-3083.
- 674 51. Xu, J., & Scheres, B. (2005). Dissection of Arabidopsis ADP-RIBOSYLATION
675 FACTOR 1 function in epidermal cell polarity. Plant Cell 17,525-36.
- 676 52. Luschnig, C., Gaxiola, R. A., Grisafi, P., & Fink, G. R. (1998). EIR1, a root-
677 specific protein involved in auxin transport, is required for gravitropism in
678 *Arabidopsis thaliana*. Genes Dev. 12, 2175–2187.
- 679

A**C****B**